First Peptide-Based System of Rigid Donor–Rigid Interchromophore Spacer–Rigid Acceptor: A Structural and Photophysical Study

C. Toniolo,*[a] F. Formaggio,[a] M. Crisma,[a] J.-P. Mazaleyrat,[b] M. Wakselman,[b] C. George,[c] J. R. Deschamps,[c] J. L. Flippen-Anderson,[c] B. Pispisa,[d] M. Venanzi,[d] and A. Palleschi[e]

Abstract: The results of X-ray diffraction analysis, fluorescence experiments and molecular mechanics calculations on the terminally protected hexapeptide -(*S*)Bin-Ala-Aib-TOAC-$(Ala)_2$- are presented. This is the first peptide investigated photophysically that is characterized by a) a rigid, binaphthyl-based α-amino acid (Bin) fluorophore, b) a rigid interchromophore bridge, the -Ala-Aib- sequence, and c) a rigid, nitroxide-based α-amino acid quencher (TOAC). In the crystal state the backbone of the spectroscopically critical 1–4 segment of both independent molecules in the asymmetric unit of the hexapeptide is folded in a regular, left-handed 3_{10}-helix. The steady-state fluorescence spectra show a remarkable quenching of Bin emission by the TOAC residue located one complete turn of the helix apart. Time-resolved fluorescence measurements exhibit a biexponential decay with solvent-dependent lifetime components ranging from 0.5 to 1.5 ns and from 3 to 5 ns. Time-decay data combined with molecular mechanics calculations allowed us to assign these lifetimes to two left-handed 3_{10}-helical conformers in which an intramolecular electronic energy transfer from excited Bin to TOAC takes place. For a given solvent the difference between the two lifetimes primarily depends on a different relative orientation of the two chromophores in the conformers, which is in turn related to a different puckering of the TOAC cyclic system.

Keywords: conformation analysis · fluorescence spectroscopy · molecular modeling · peptides · structure elucidation

Introduction

Rigid donor–spacer–acceptor systems provide well-defined distances and orientations between appropriate probes, thus greatly facilitating a reliable and correct interpretation of experimental results based on the geometrical dependence of photophysical processes.[1, 2] Peptide-based systems of different lengths present a remarkable advantage over derivatized polycyclic hydrocarbon skeletons, because they are very easily synthetically assembled.

Oligopeptide helices of variable length have already been used as spacers in photophysical studies. Following this approach, distance dependences of energy[3] and electron transfer[4] have been examined. However, particularly in the case of relatively short peptides, only a restricted mobility has been achieved. The most commonly used oligopeptide series in this context are $(\text{L-Pro})_n$, followed by $(\text{Gly})_n$, $(\text{L-Ala})_n$, and γ-substituted $(\text{L-Glu})_n$. Extensive investigations on $(\text{L-Pro})_n$ oligomers have clearly shown that different populations of multiple conformers arise from *cis* $\rightleftharpoons$ *trans* (ω torsion angle) and *cis*′ $\rightleftharpoons$ *trans*′ (ψ torsion angle) equilibria.[5] On the other hand, $(\text{Gly})_n$ oligomers are known to fold in the ternary helix poly$(\text{Gly})_n$ I, or in the antiparallel β-sheet conformation

[a] Prof. C. Toniolo, Dr. F. Formaggio, Dr. M. Crisma
Department of Organic Chemistry, University of Padova
Via Marzolo 1, I-35131 Padova (Italy)
Fax: (+39) 049-827-5239
E-mail: biop02@chor.unipd.it

[b] Dr. J.-P. Mazaleyrat, Dr. M. Wakselman
SIRCOB, Bât. Lavoisier, University of Versailles
F-78000 Versailles (France)
Fax: (+33) 1-3925-4452

[c] Dr. C. George, Dr. J. R. Deschamps, Dr. J. L. Flippen-Anderson
Laboratory for the Structure of Matter
Naval Research Laboratory
Washington, DC 20375 (USA)
Fax: (+1) 202-767-6874

[d] Prof. B. Pispisa, Prof. M. Venanzi
Department of Chemical Sciences and Technologies
University of Rome Tor Vergata
I-00133 Rome (Italy)
Fax: (+39) 06-2020-420

[e] Prof. A. Palleschi
Department of Chemistry,
University of Rome La Sapienza
I-00185 Rome (Italy)
Fax: (+39) 06-490-631

0947-6539/99/0508-2254 $ 17.50+.50/0

Abstract in Italian: *In questo lavoro vengono presentati i risultati di un'analisi con la diffrazione dei raggi X, di esperimenti di fluorescenza e di calcoli di meccanica molecolare sull'esapeptide N- e C-protetto -(S)-Bin-Ala-Aib-TOAC-(Ala)$_2$-. Questo è il primo peptide che viene studiato con metodi fotofisici che sia caratterizzato da: a) un α-amminoacido fluorescente (a base binaftilica) rigido (Bin); b) uno spaziatore intercromoforico, la sequenza -Ala-Aib-, rigido, e c) un α-amminoacido quencher (a base nitrossilica) rigido (TOAC). Allo stato cristallino lo scheletro del segmento 1–4, critico dal punto di vista spettroscopico, di entrambe le molecole indipendenti nell'unità asimmetrica dell'esapeptide forma un'elica 3_{10} sinistrogira regolare. Gli spettri di fluorescenza statica evidenziano un notevole quenching dell'emissione del Bin da parte del residuo di TOAC situato dopo un giro completo dell'elica. Misure di fluorescenza dinamica mostrano andamenti con decadimenti biesponenziali con componenti con tempi di vita da 0.5 e 1.5 ns a da 3 a 5 ns. Questi valori variano al variare del solvente. I dati di fluorescenza, combinati con quelli dei calcoli di meccanica molecolare, ci hanno consentito di assegnare i tempi di vita a due conformeri 3_{10}-elicoidali sinistrogiri in entrambi i quali ha luogo un trasferimento di energia intramolecolare dal Bin eccitato al TOAC. Per un dato solvente la differenza tra i due tempi di vita dipende principalmente dalla diversa orientazione relativa dei due cromofori in ciascun conformero, la quale è a sua volta collegata al diverso corrugamento del sistema ciclico del residuo di TOAC.*

Abstract in French: *Dans l'article sont présentés les résultats d'une analyse de diffraction aux rayons X, des expériences de fluorescence et des calculs de mécanique moléculaire concernant l'hexapeptide -(S)Bin-Ala-Aib-TOAC-(Ala)$_2$- dont les deux extrémités sont protégées. C'est le premier peptide examiné jusqu'` présent du point de vue photophysique, caractérisé par: a) un fluorophore α-amino acide binaphthylique (Bin) rigide, b) un lien interchromophore, la séquence -Ala-Aib-, rigide, et c) un extincteur de fluorescence α-amino acide nitroxyde (TOAC) rigide. A l'état cristallin, le squelette du segment 1–4, spectroscopiquement crucial, des deux molécules indépendantes dans l'unité asymétrique, est replié en forme d'hélice 3_{10} régulière. Les spectres de fluorescence à l'état stationnaire montrent une extinction remarquable de l'émission du Bin par le résidu TOAC situé un tour complet d'hélice plus loin. Les mesures de fluorescence en fonction du temps présentent une décroissance biexponentielle avec des durées de vie dépendantes du solvant, dont les composantes sont dans les intervalles 0.5 à 1.5 ns et 3 à 5 ns. Les calculs de mécanique moléculaire nous ont permis d'attribuer ces durées de vie à deux conformères hélicoïdaux 3_{10} gauches dans lesquels un transfert intramoléculaire d'énergie électronique, de l'état excité de Bin au résidu TOAC, a lieu. Pour un solvant donné, la différence entre les deux durées de vie dépend principalement de l'orientation relative des deux chromophores dans les conformères, laquelle est à son tour liée à une géométrie différente du système cyclique du résidu TOAC.*

poly(Gly)$_n$ II,[6] while (L-Ala)$_n$ and γ-substituted (L-Glu)$_n$ oligomers may adopt either the α-helical or the β-sheet conformation.[6a, 7] In addition, statistically disordered forms occur largely in the complex conformational equilibria of short oligopeptides from C^{α}-trisubstituted (proteinogen) amino acids, with their total population inversely proportional to the peptide main chain length.

As it is clear none of the peptide series discussed above can produce truly rigid spacers, in the last few years we have concentrated our efforts on oligomeric series rich in the structurally restricted C^{α}-tetrasubstituted α-amino acids. After careful investigations of model peptides in both solution and crystal state, we[8] and others[9] have found that in peptides rich in Aib (α-aminoisobutyric acid) (Figure 1), the prototype

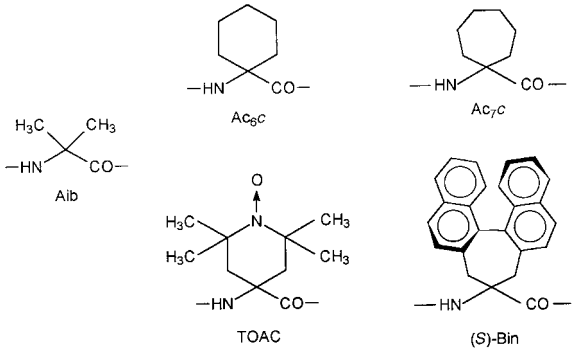

Figure 1. Chemical structures of the five $C^{\alpha,\alpha}$-disubstituted glycines discussed in this work.

of this family of amino acids, and in its Ac_nc (1-aminocycloalkane-1-carboxylic acid) cyclic analogues, stable type-III (III′) β-turns,[10] regular 3_{10}-helices,[11] or α-helices are formed. This largely depends on the main chain length and Aib (or Ac_nc) content.[8, 9b] Stimulating results from this approach have already been reported by several groups.[12–15]

However, almost all of these investigations have exploited as photoprobes a) flexible, unmodified, proteinogen amino acids (Trp, Tyr, Met) or b) flexible, appropriately side-chain-modified, proteinogen amino acids (Cys, Lys, Glu, Ala, Pro, Phe). To our knowledge, the only notable exceptions are an Ac_6c-based, constrained Trp residue, which, however, has not yet been incorporated into peptides,[16] and further two aromatic homologues of Ac_nc, which have been inserted into a 3_{10}-helical structure, but in the relative positions *i* and *i*+2, after only part of one turn of the ternary helix.[12e, f]

In this article we report the results of our structural (X-ray diffraction) analysis of the hexapeptide Boc-(*S*)-Bin-Ala-Aib-TOAC-(Ala)$_2$-O*t*Bu (Boc, *tert*-butyloxycarbonyl; Bin, 2′,1′:1,2;1″,2″:3,4-dinaphthcyclohepta-1,3-diene-6-amino-6-carboxylic acid; TOAC, 2,2,6,6-tetramethylpiperidine-1-oxyl-4-amino-4-carboxylic acid; O*t*Bu, *tert*-butoxy) in combination with data of steady-state and time-resolved fluorescence experiments and molecular mechanics calculations. This peptide system is characterized by: a) a rigid donor, (*S*)-Bin, an axially dissymmetric (atropoisomeric), 1,1′-binaphthyl side-chain-substituted Ac_7c;[17] b) a rigid, Aib-based, 3_{10}-helical interchromophore bridge, and c) a rigid, achiral, α-amino acid acceptor, TOAC, an Ac_6c analogue containing a

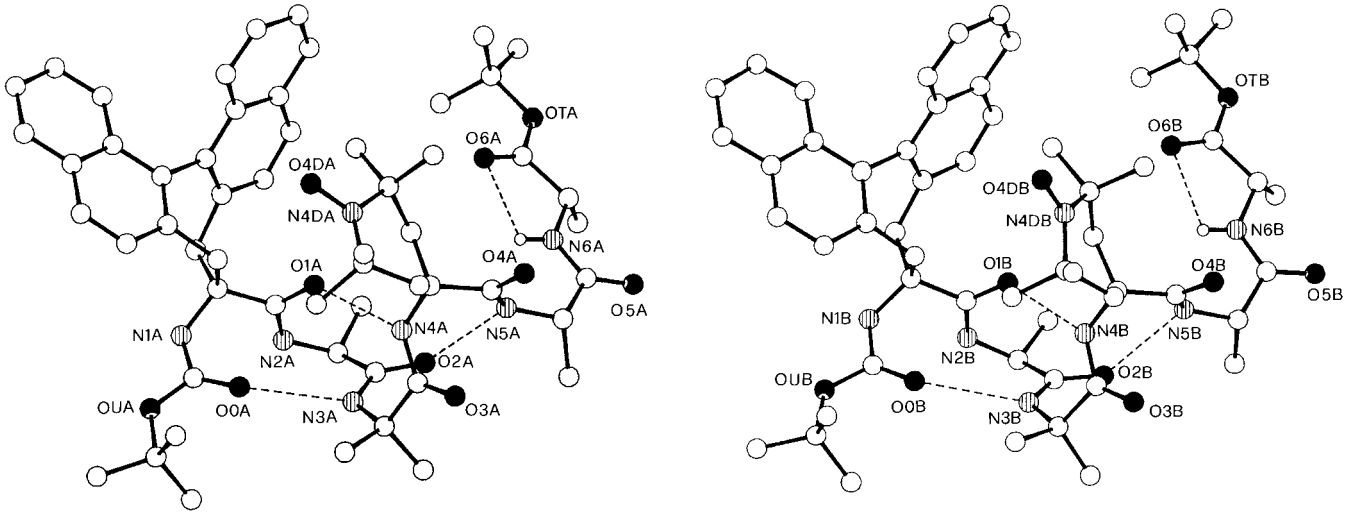

Figure 2. X-ray diffraction structures of the two independent molecules **A** and **B** in the asymmetric unit of the Bin–TOAC hexapeptide. Nitrogen and oxygen atoms are labeled. The intramolecular C=O···H–N H-bonds are represented by dashed lines.

Table 1. Relevant backbone torsion angles [°] with their esd's for the two independent molecules **A** and **B** in the asymmetric unit of the Bin–TOAC hexapeptide.

Torsion angle	Mol. **A**	Mol. **B**
θ^1	−177.2(4)	−168.9(3)
ω_0	159.6(4)	162.8(3)
ϕ_1	55.7(5)	59.7(5)
ψ_1	44.5(5)	32.9(5)
ω_1	171.7(4)	177.0(4)
ϕ_2	56.3(5)	52.5(5)
ψ_2	32.7(5)	34.5(5)
ω_2	177.1(4)	176.6(4)
ϕ_3	56.4(5)	58.1(6)
ψ_3	19.0(5)	23.6(6)
ω_3	−179.8(3)	176.6(4)
ϕ_4	50.3(5)	59.6(5)
ψ_4	36.2(5)	34.9(5)
ω_4	−174.4(4)	−174.0(4)
ϕ_5	−109.1(5)	−89.0(5)
ψ_5	−2.0(6)	−17.9(6)
ω_5	−176.9(5)	−172.6(4)
ϕ_6	−168.7(5)	−171.9(4)
ψ_6	−177.8(5)	−175.6(4)
ω_6	170.4(6)	170.1(4)

stable nitroxide free radical.[15] Appropriately substituted naphthalene derivatives and nitroxide-containing compounds are efficient fluorophores and fluorescence quenchers. The Bin and TOAC residues were incorporated in relative positions i and $i+3$, that is, after one complete turn of the 3_{10}-helix, to achieve an efficient spatial overlap of the two chromophores.

Results and Discussion

Crystal structure: The X-ray diffraction structures of the two independent molecules **A** and **B** in the asymmetric unit of Boc-(*S*)-Bin-Ala-Aib-TOAC-(Ala)$_2$-O*t*Bu are depicted in Figure 2. Relevant backbone torsion angles[18] are listed in Table 1. In Table 2 the intra- and intermolecular H-bond parameters are given.

Bond lengths and bond angles (deposited at CCDC, see Experimental Section) are in good agreement with previously reported values for the geometry of the Boc-urethane[19] and -O*t*Bu ester[20] groups, the peptide unit,[21] and the Bin,[17a] Aib,[22] and TOAC[15a, d, e] residues. In particular, the N^{δ}–O^{δ} bond lengths of the TOAC nitroxide group (1.302(5) Å for molecule **A** and 1.294(7) Å for molecule **B**), the external O^{δ}-N^{δ}-C^{γ} bond angles [in the range 116.7(4)°–118.3(5)°], and the internal bond angle at the N^{δ} atom [125.0(4)° for molecule **A** and 124.0(4)° for molecule **B**] compare well with those published for other TOAC residues.[15a, d, e] A similar conclusion may be drawn for the length of the characteristic C–C bond joining the two naphthyl moieties of Bin [1.499(6) Å for molecule **A** and 1.493(6) Å for molecule **B**].[17a]

Table 2. Intra- and intermolecular hydrogen bond parameters for the two independent molecules **A** and **B** in the asymmetric unit of the Bin–TOAC hexapeptide.

Type of H-bond	Donor D	Acceptor A	Symmetry operation	Distance [Å] D···A	Distance [Å] H···A	Angle [°] D-H···A
Intramolecular						
Mol. **A**	N3-H	O0	*x, y, z*	2.993(5)	2.24	146
	N4-H	O1	*x, y, z*	2.978(4)	2.14	166
	N5-H	O2	*x, y, z*	3.116(5)	2.31	157
	N6-H	O6	*x, y, z*	2.630(6)	2.24	108
Mol. **B**	N3-H	O0	*x, y, z*	2.995(5)	2.20	155
	N4-H	O1	*x, y, z*	2.977(5)	2.15	163
	N5-H	O2	*x, y, z*	3.120(6)	2.38	145
	N6-H	O6	*x, y, z*	2.645(5)	2.26	107
Intermolecular						
	N1A-H	O5A	$-1+x, y, z$	2.946(5)	2.26	137
	N2A-H	O3B	$-1+x, y, z$	2.890(5)	2.30	127
	N1B-H	O5B	$-1+x, y, z$	2.988(6)	2.31	136
	N2B-H	O4DA	$1-x, -1/2+y, 2-z$	2.801(7)	2.05	146

0947-6539/99/0508-2256 $ 17.50+.50/0 *Chem. Eur. J.* **1999**, *5*, No. 8

The conformational differences between molecules **A** and **B** are of minor significance. The -(*S*)-Bin[1]-Ala-Aib-TOAC[4]- sequence of both independent molecules is folded into a regular, left-handed 3_{10}-helix with average φ, ψ torsion angles 54.7°, 33.1° for molecule **A** and 57.5°, 31.5° for molecule **B**. The helical structure is stabilized by three successive $1 \leftarrow 4$ C=O···H–N intramolecular hydrogen bonds of the β-turn(C_{10})-III type.[10] The range of observed N···O distances is 2.978(4) Å – 3.120(6) Å; in both molecules the weaker hydrogen bond[23] is that joining the (peptide) N5–H··· O2=C′2 (peptide) groups. In both molecules the Ala[5] residue is found in the right-handed bridge region of the φ, ψ space.[24] Interestingly, again for both molecules, the C-terminal Ala[6] residue is fully extended, producing an unusual $2 \rightarrow 2$ (or C_5) N6–H···O6=C′6 intramolecularly hydrogen-bonded structure.[8, 25]

The deviation of the urethane, peptide, and ester ω torsion angles from the ideal value of the *trans* planar conformation (180°) is significant ($|\omega| \geq 10°$) only at the two ends of the peptide chain, namely for the urethane ω_0 and ester ω_6 angles. The conformation of the Boc-urethane group (θ^1 and ω_0 torsion angles) is the usual *trans, trans* or type-*b* conformation.[19] The ester disposition with respect to the preceding C$^\alpha$6–N6 bond is close to the synperiplanar conformation.[26] The *tert*-butyl ester groups of the -O*t*Bu and Boc- moieties are in a conformation in which the three methyl substituents of the quaternary carbon atom are staggered with respect to the -C$^\alpha$6-C′6(=O6)-OT and N1-C′0(=O0)-O_u- planes, respectively, as usually found in ester groups from tertiary alcohols.[20]

The TOAC residue in molecule **A** differs from that in molecule **B** in the puckering of the piperidine ring. This six-membered cyclic system is close to the boat conformation in molecule **A**, with the puckering parameters[27] $Q_T = 0.607(6)$ Å, $\Theta_2 = 91.2(5)°$, $\Phi_2 = 294.8(5)°$, whereas it adopts the twist-boat conformation in molecule **B**, with the puckering parameters $Q_T = 0.621(6)$ Å, $\Theta_2 = 93.4(5)°$, $\Phi_2 = 274.0(5)°$. As a consequence, small but significant differences are found in the orientation of the substituents relative to the normal to the piperidine ring average plane. More specifically, the angle between the normal to the average plane and the C$^\alpha$4–N4 bond is 21.8(3)° in molecule **A**, while 32.1(3)° in molecule **B**. Furthermore, the angle between the normal to the average plane and the C$^\alpha$4–C′4 bond is 51.8(3)° in molecule **A**, while it is 42.8(3)° in molecule **B**. These values correspond to a slightly different orientation of the TOAC average plane with respect to the peptide backbone. Also, the nitroxide N4D–O4D bond is shifted in one molecule compared with the other by the different TOAC puckering. This bond is perfectly equatorial (the angle with the normal to the TOAC average plane is 90.0(4)°) in molecule **B**, while this angle is 79.4(4)° in molecule **A**.[15a, d, e]

In the Bin residue of both molecules the α-amino substituent is halfway between the axial and equatorial dispositions with respect to the average plane of the seven-membered ring. Again for both molecules, this cyclic system shows a twist-boat conformation[28] with the following puckering parameters: $Q_T = 1.113(4)$ Å, $\Theta_2 = 84.5(2)°$, $\Phi_2 = 268.5(2)°$, $\Phi_3 = 261(3)°$ for molecule **A**, and $Q_T = 1.115(4)$ Å, $\Theta_2 = 84.9(3)°$, $\Phi_2 = 268.5(2)°$, $\Phi_3 = 261(3)°$ for molecule **B**. A similar conformation of the Bin seven-membered ring was recently reported for the free amino acid.[17a] Each naphthyl moiety is substantially planar, the largest deviation from planarity for carbon atoms in each moiety being in the range ±0.026(4) Å – 0.070(6) Å. The dihedral angles between normals to the average planes of naphthyl···naphthyl′, naphthyl ···TOAC and naphthyl′···TOAC have values of 62.7(1)°, 58.8(1)°, 24.9(1)°, respectively, for molecule **A**, while they are 64.6(1)°, 57.6(1)°, 44.7(1)° for molecule **B**. The angles between the nitroxide bond and the normals to the average planes of the two naphthyl moieties are 53.7(3)°, 80.8(3)° for molecule **A**, and 70.4(3)°, 52.3(4)° for molecule **B**. The distance between the C$^\alpha$ atoms of Bin[1] and TOAC[4], after one complete turn of the 3_{10}-helix,[11] is 5.876(6) Å in molecule **A** and 5.779(6) Å in molecule **B**. The shortest intramolecular (TOAC nitroxide) O···C (Bin aromatic) distance is 4.502(7) Å in molecule **A** and 5.039(9) Å in molecule **B**. In addition, in each molecule **A** and **B** one TOAC methyl group is directed toward the center of the external phenyl ring of one binaphthyl moiety; the corresponding (methyl) C···C (phenyl) separations being in the ranges of 3.509(7) Å – 3.861(7) Å and 3.586(9) Å – 3.727(8) Å, respectively.

In the crystal rows of each of the two independent molecules **A** and **B** are formed along the *a* direction by N1–H···O5=C′5 intermolecular hydrogen bonds. These rows are linked into columns by N2A–H···O3B=C′3B intermolecular hydrogen bonds. The columns are connected into a continuous 3D network by an N2B–H···O4DA hydrogen bond, which links molecules around a crystallographic screw axis. The solvent (acetone) molecules lie in channels along the *a* direction and do not interact with the peptide molecules.

Ground- and excited-state behaviors: The UV absorption spectra of the Bin derivative (blank) and the Bin – TOAC hexapeptide in methanol (MeOH) solution are shown in Figure 3. They exhibit a shift to 305 nm of the naphthalene

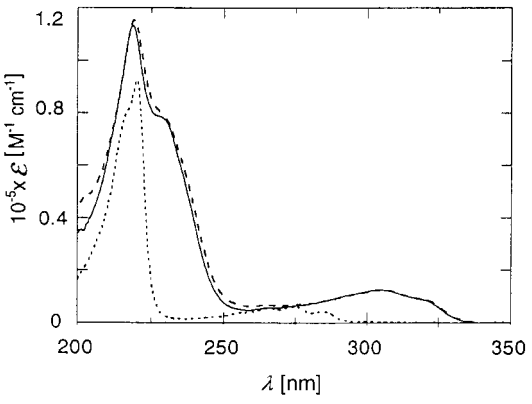

Figure 3. UV absorption spectra of the Bin derivative (full line), the Bin – TOAC hexapeptide (dashed line) and naphthalene (dotted line) in MeOH solution.

band at 280 nm, while the band at about 225 nm is doubled, and the maxima being found at 220 nm and 232 nm. According to Förster[29] this finding implies a strong electronic coupling of the naphthyl (N) moieties in the ground state through intramolecular exciton interaction, and at the same time a much larger rate of excitation transfer between the

chromophores in the binaphthyl group than the frequency of molecular vibrations.[30] As a result, the exciton is delocalized over the entire binaphthyl group. Accordingly, the CD spectrum within the 200–300 nm wavelength region (not shown) exhibits an exciton splitting clearly ascribable to the aforementioned coupling regime.

The presence of TOAC in the molecule does not perturb such a strong coupling effect, since the absorption and CD spectra of the Bin–TOAC hexapeptide are almost identical to those of the Bin derivative. This result is indicative of a severe conformational restriction that prevents the overlap of the electron density distributions of the probes. In addition, no charge transfer bands are present in the spectrum of the Bin–TOAC hexapeptide, which rules out the formation of a ground-state charge-transfer (CT) complex.[31]

Although the dielectric constant of the solvent may affect the resonance interaction by altering the oscillator strength of the transition, no significant variation of the spectra could be observed by changing solvent. This lack of solvent effects is presumably connected with the strong electronic coupling between the two naphthyl moieties in the Bin chromophore.[30]

We next examined the excited-state behavior of the Bin–TOAC hexapeptide. Despite the extensive literature aimed at understanding the mechanism through which excited states are quenched by paramagnetic species, such as a nitroxyl radical, there is not yet a univocal interpretation of this phenomenon, partly because of the sparseness of the experiments. Indeed, most of the literature on nitroxide-based quenchers concerns noncovalently linked fluorophore-quencher dyads, leading to measured quenching rate constants controlled by diffusion processes.[32a, 33a] Consequently, the issue of a detailed quenching mechanism by a nitroxide group, with specification of its distance and orientation dependence in covalently linked donor–acceptor dyads, must be considered still unsettled, in spite of the widespread use of doublet quenchers to probe the structural and dynamic features of membranes,[34] micelles,[35] and protein surfaces.[32]

It is generally accepted that in freely diffusive systems a major pathway of singlet-state quenching by a nitroxide would either be an intersystem crossing to the triplet state induced by electron exchange[32a, 36] or a catalyzed internal conversion to the ground state;[33] the mechanisms are exclusive. In other instances, however, charge transfer, electron transfer[32c] or Förster[37] energy transfer[32b, 34f] were found to play an important role. Calculations based on measured spectral properties showed that Förster transfer mechanism extends the nitroxide quenching radius to as much as 10 Å,[34f] so that the range of the induced quenching is considerably over what it would be with only vibrational coupling or enhanced intersystem crossing. On the other hand, Dexter energy transfer[38] may also hold, but it requires singlet energies ($E_{00,\,\mathrm{Bin}} = 3.73$ eV) greater than the lowest excited state energy of the nitroxide, which in the case of TOAC is approximately 3.1 eV, besides a short center-to-center distance, less than, say, 4 Å.

Steady-state fluorescence spectra ($\lambda_{ex} = 305$ nm) in MeOH or dioxane show a substantial quenching of N singlet emission by TOAC, as illustrated in Figure 4. No evidence for exciplex emission from the Bin–TOAC hexapeptide could be obtained, even by decreasing solvent polarity. The fluorescence quantum yield of the peptide (Φ) in a number of solvents with different polarity, and the efficiency of the quenching process, E, as given by $[1 - (\Phi/\Phi_0)]$, where Φ_0 is the quantum yield of the blank, are reported in Table 3. Rather surprisingly, the quenching efficiency from steady-state measurements varies only slightly when the solvent is changed.

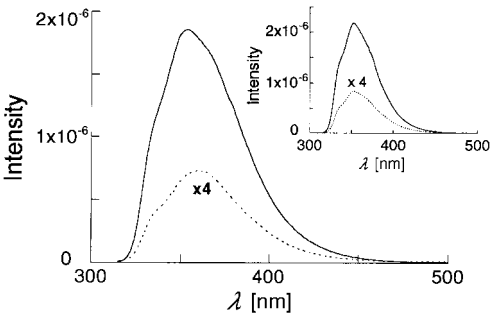

Figure 4. Fluorescence spectra of the Bin derivative (full line) and the Bin–TOAC hexapeptide (dashed line) in MeOH solution. Inset: same spectra in dioxane solution.

Table 3. Quantum yields and energy transfer efficiencies for the Bin–TOAC hexapeptide from steady-state fluorescence measurements.

Solvent	ε_r[a]	Φ_0[b]	Φ[c]	E[d]
1,4-Dioxane	2.2	0.77	0.07	0.91
Ethyl acetate	6.0	0.74	0.04	0.95
1-Butanol	17.1	0.72	0.06	0.92
Isopropanol	18.3	0.75	0.04	0.95
Ethanol	24.3	0.76	0.05	0.93
Methanol	32.6	0.71	0.07	0.90

[a] Dielectric constant [25 °C]. [b] Quantum yield of the blank (Bin derivative). [c] Quantum yield of the Bin–TOAC hexapeptide. [d] Energy transfer efficiency, $E = 1 - (\Phi/\Phi_0)$.

As far as the time decay measurements ($\lambda_{ex} = 305$, $\lambda_{em} = 360$ nm) are concerned, the decay curve of the blank was found to be strictly monoexponential, with τ_0 ranging from 3.6 to 4.9 ns, depending on the solvent (Table 4). It is definitely shorter than that of naphthalene, $\tau_N = 52.5 \pm 0.7$ ns, thereby indicating a strong dynamic quenching, ascribable to an exciton interaction associated with the aforementioned coupling regime. Instead, the Bin–TOAC hexapeptide decays biexponentially [Eq. (1), where $i = 1$ or 2]. Typical examples

$$I(t) = \Sigma_i \alpha_i \exp(-t/\tau_i) \quad (1)$$

Table 4. Fluorescence lifetimes and efficiencies for the Bin–TOAC hexapeptide in different solvents.[a]

Solvent	τ_0[b] [ns]	α_1	τ_1 [ns]	E_1[c]	α_2	τ_2 [ns]	E_2[d]	χ^2
1,4-Dioxane	3.62	0.55	0.84	0.77	0.45	3.06	0.15	1.28
Ethyl acetate	3.95	0.59	0.95	0.73	0.41	3.48	0.09	1.14
1-Butanol	4.12	0.63	0.68	0.83	0.37	3.15	0.24	0.99
Isopropanol	4.12	0.79	0.53	0.87	0.21	3.25	0.21	1.19
Ethanol	4.55	0.75	1.01	0.78	0.25	3.90	0.15	1.13
Methanol	4.89	0.79	1.36	0.72	0.21	4.46	0.07	1.33

[a] $\lambda_{ex} = 305$ nm, $\lambda_{em} = 360$ nm. The uncertainty in lifetimes is lower than 10%, while that of the preexponents is about 20%. [b] Fluorescence time decay of the blank. [c] From Equation (2). The uncertainty is about 10%. [d] From Equation (2). The uncertainty is about 30%.

0947-6539/99/0508-2258 $ 17.50+.50/0 *Chem. Eur. J.* **1999**, *5*, No. 8

of decay curves for the Bin derivative and the Bin – TOAC hexapeptide in ethanol (EtOH) are presented in Figure 5. In all cases, no significant change was observed on varying the sample concentration within one order of magnitude ($1 \cdot 10^{-6} - 2 \cdot 10^{-5}$ M), so that intermolecular effects can be ruled out.

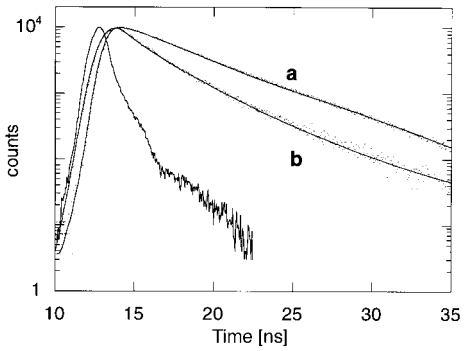

Figure 5. Typical examples of fluorescence decay. Normalized decay profile ($\lambda_{ex} = 305$ nm, $\lambda_{em} = 360$ nm) for the Bin derivative a) and the Bin – TOAC hexapeptide b) in EtOH solution. The full lines represent the best fit to the experimental data by a monoexponential a) and a biexponential b) decay. The lamp profile is also shown.

The short decay time, τ_1, ranges from 0.5 to 1.4 ns and the longer one, τ_2, from 3.1 to 4.5 ns, depending on the solvent. A lifetime distribution analysis confirms these findings, because it gives one distribution for Bin and two narrow distributions for Bin – TOAC. Therefore, we are inclined to assign these lifetimes to two highly populated, low-energy conformers that exhibit both a different center-to-center distance and mutual orientation of the chromophores, in agreement with the molecular mechanics data reported below.

Two experimental results confirm this assignment. First, temperature-dependent, time-resolved fluorescence experiments show that the preexponents of the two time decay components remain practically the same from 290 K to 330 K, thereby emphasizing the severe conformational restriction of the compound. Secondly, the distribution analysis of the fluorescence time decay in dimethyl sulfoxide (DMSO), a solvent of well-known disruptive effects on peptide ordered secondary structures, gives rise to one wide distribution only, very likely arising from many slightly different conformations.

Table 4 lists lifetimes, preexponents and efficiencies in a number of solvents; the transfer efficiency is given by Equation (2).

$$E_i = 1 - (\tau_i/\tau_0) \tag{2}$$

We then addressed the problem of the mechanisms that could contribute to the singlet state quenching in the Bin – TOAC hexapeptide. In principle, the rate constant for intramolecular quenching of binaphthyl, (N,N)*, by the nitroxide moiety is the sum of rate constants for each potential relaxation pathway as given in Equation (3); for $i = 1$ or 2, $k_{i,(N,N)^*}$ is given by Equation (4).

$$k_{i,(N,N)^*} = k_{F,i} + k_{D,i} + k_{et,i} + k_{ex,i} \tag{3}$$

$$k_{i,(N,N)^*} = (\tau_i^{-1} - \tau_0^{-1}) \tag{4}$$

Equation (3) involves the rate constants for quenching by Förster and Dexter energy transfer, electron transfer, and electron exchange through the local relaxation of the singlet state, while the rate constant for quenching by CT is not incorporated because of the lack of CT absorption or emissive components.

According to the dipole – dipole interaction model, the rate constant for Förster energy transfer can be expressed by Equation (5). J_F is the overlap integral calculated from fluorescence spectra, as obtained by Equation (6) and listed

$$k_{F,i} = 8.71 \cdot 10^{23} \cdot (J_F \kappa_i^2 \Phi_0)/(R_i^6 n^4 \tau_0) \tag{5}$$

$$J_F = \frac{\int_0^\infty F_D(\bar{\nu}) \varepsilon_A(\bar{\nu}) \bar{\nu}^{-4} d\bar{\nu}}{\int_0^\infty F_D(\bar{\nu}) d\bar{\nu}} \tag{6}$$

in Table 5 for the different solvents used, κ_i^2 the orientation parameter of the probes [Eq. (7)], Φ_0 the quantum yield of the Bin derivative, R_i the interprobe separation distance and n the refractive index of the solvent.

Table 5. Förster (J_F) and Dexter (J_D) spectral overlap integral, and Förster radius (R_0) for the Bin – TOAC hexapeptide in different solvents.

Solvent	$10^{18} J_F$ [cm^3 mol^{-1}][a]	$10^5 J_D$ [cm][b]	R_0 [Å][c]
1,4-Dioxane	13.2	4.38	10.5
Ethyl acetate	19.9	5.40	11.5
1-Butanol	8.6	3.31	9.9
Isopropanol	4.5	2.22	9.0
Ethanol	6.2	6.48	9.5
Methanol	6.1	2.85	9.7

[a] From Equation (6). [b] From Equation (10). [c] From Equation (13).

In Equation (6), F_D ($\bar{\nu}$) is the fluorescence intensity of the donor (Bin) and ε_A ($\bar{\nu}$) the extinction coefficient of the acceptor (TOAC) at wavenumber ($\bar{\nu}$). On the other hand, the relative orientation of the chromophores, when they do not rotate fast enough to randomize their orientation during the donor lifetime, can be determined[39, 40a] by Equation (7).

$$\kappa_i^2 = \cos^2\theta(3\cos^2\gamma + 1) \tag{7}$$

In such a case, a particular relative orientation between the donor and acceptor molecules is described by two angles only, as shown in Figure 6, where the geometry for evaluating the orientation in space of the transition dipole moments of the acceptor and donor moieties[39] is illustrated. R' is the distance between the center of mass of Bin* and TOAC, the transition dipole moment of TOAC lying in the CNC plane[36b] and perpendicular to the N–O bond, while that of the binaphthyl is a vectorial combination of the dipoles from each naphthalene group. In addition, γ is the angle that the Bin* transition dipole moment makes with the line joining the center of mass of Bin* and TOAC, E is the vector representing the electric field at the center of mass of TOAC induced by the transition dipole moment of Bin*, and θ the angle between E and the transition dipole moment of TOAC.[39, 40a] In the same figure the total dipole moment of the 3_{10}-helical backbone chain is also shown. It is known[41] that the helical dipole moment generates an electrostatic potential directed from the N-ter-

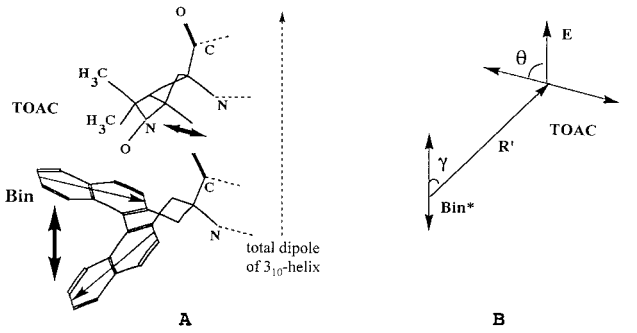

Figure 6. Schematic representation of the two chromophores in the Bin–TOAC hexapeptide: A) with their electric dipole transition moments (heavy double arrows); B) with the angles defining the orientation between the transition dipole moments of the donor and acceptor molecules, and the electric field vector generated by Bin* acting at the center of mass of the TOAC moiety.

minus to the C-terminus of the peptide chain; this could affect the coupling of the transition moments of the two probes.[13] In our case, however, we will demonstrated that such an effect is definitely minor.

The efficiency in the Dexter energy transfer mechanism is exponentially dependent on the interchromophoric distance as given in Equation (8), where $i=1$ or 2, $k_D=\tau_0^{-1}$ is the rate constant for the donor emission, and J_D is the Dexter overlap integral, obtained by spectroscopic measurements and reported in Table 5 for the different solvents used.

$$E_i/(1-E_i)=(2\pi/k_D\hbar)V_i^2J_D \tag{8}$$

The electronic matrix coupling element V_i^2 is defined in Equation (9), where a is the average Bohr radius (0.625 Å[42]) and K_i is a quantity with dimensions of energy, corresponding to the electronic matrix coupling at orbital contact. The Dexter overlap integral is given in Equation (10) and in Equation (11) under normalization conditions.

$$V_i^2=K_i\exp(-2R_i/a) \tag{9}$$

$$J_D=\int_0^\infty F_{i,D}(\bar{\nu})\varepsilon_{i,A}(\bar{\nu})d\bar{\nu} \tag{10}$$

$$\int_0^\infty F_D(\bar{\nu})d\bar{\nu}=\int_0^\infty \varepsilon_A(\bar{\nu})d\bar{\nu}=1 \tag{11}$$

Both Förster and Dexter models predict that for a given donor–acceptor distance and orientation the rate constants for transfer will increase linearly with increasing values of the spectral overlap integrals, J_F and J_D, respectively. This is indeed the case for the plot of log $k_{F,i}$ against log J_F, as in Figure 7. Both the values of Φ_0, τ_0 and n in a given solvent, and the values of R_i and κ_i^2 listed in Table 6 were used to evaluate $k_{F,i}$, these latter parameters being obtained by molecular mechanics calculations (see next Section), in which the appropriate dielectric constant of the solvent was used in the electrostatic term. By contrast, a plot of log $k_{D,i}$ against log J_D does not give such a relationship, as illustrated in Figure 8. These findings strongly suggest that, on the nanosecond time scale, a Förster transfer mechanism is the major pathway for Bin quenching by TOAC. Consistently, evaluation of the electronic matrix coupling at orbital contact, K_i [Eq. (9)], in the six solvents used leads to the following average values

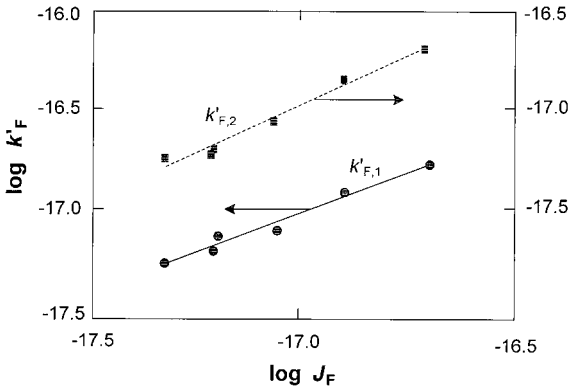

Figure 7. Intramolecular quenching constant against Förster spectral overlap integral, J_F [cm^3 mol^{-1}], in different solvents (listed in Table 5) for the Bin–TOAC hexapeptide. The rate constants have been normalized [$k'_{F,i}=(k_{i,(N,N)^*}\tau_0R_i^6n^4)/\kappa_i^2\Phi_0(9.77\cdot10^3)^6$; the last figure is the conversion factor (when R_i is in Å)], to account for lifetime, quantum yield and refractive index dependence on solvent medium.

Table 6. Molecular parameters and calculated efficiencies of the two most stable conformers[a] of the Bin–TOAC hexapeptide in different solvents.

Solvent	R_1[Å]	κ_1^2[b]	R_2[Å]	κ_2^2[b]	$E_{1,calc}$[c]	$E_{2,calc}$[c]
1,4-Dioxane	5.91	0.072	6.12	0.0055	0.773	0.174
Ethyl acetate	6.01	0.055	6.13	0.0045	0.802	0.227
1-Butanol	5.93	0.170	6.18	0.0150	0.847	0.275
Isopropanol	5.87	0.300	6.15	0.0160	0.854	0.191
Ethanol	5.98	0.150	6.19	0.0075	0.783	0.128
Methanol	5.84	0.090	6.18	0.0035	0.739	0.073

[a] As obtained by molecular mechanics calculations (Figure 10). [b] Orientation parameter; from Equation (7). [c] Calculated efficiencies, from Equation (12) to be compared with the experimental efficiencies (Table 4).

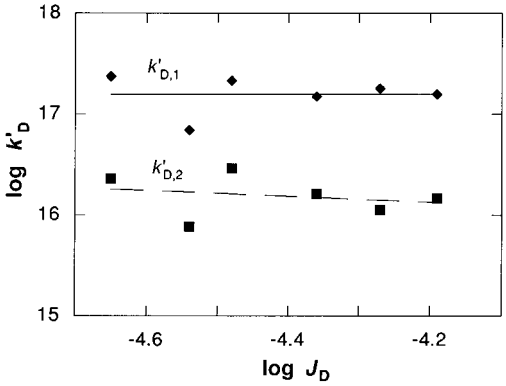

Figure 8. Intramolecular quenching constant against Dexter spectral overlap integral, J_D [cm^{-1}], under the same conditions as those in Figure 7 ($k'_{D,i}=k_{i,(N,N)^*}/\exp(-2R_i/a)$, for the Bin–TOAC hexapeptide.

$K_1=(7.8\pm4.9)\cdot10^{-7}$ and $K_2=(8.0\pm5.9)\cdot10^{-8}$ dyne, which differ by some 4–5 orders of magnitude from the values reported for electronic energy transfer by exchange interaction in bichromophoric molecules.[43] On the basis of these results, we can rule out a Dexter transfer mechanism.

We are also inclined to rule out the occurrence of electron transfer because of the lack of correlation between the solvent polarity and the energetics of the electron transfer reaction for the Bin*–TOAC redox pair, despite the favorable thermodynamic driving force for both the reductive ($\Delta G^0=-1.6$ eV) and oxidative ($\Delta G^0=-0.6$ eV) processes. In addi-

0947-6539/99/0508-2260 $ 17.50+.50/0 *Chem. Eur. J.* **1999**, *5*, No. 8

tion, two other contributors to the total reaction free energy, the coulombic attraction and the solvation of the charge separated species, are strongly solvent dependent and are expected to correlate with the observed quenching rate constants. Apparently, however, this is not the case, because of the following values: $k_1 = 5.3 \cdot 10^8\,s^{-1}$ and $k_2 = 2.0 \cdot 10^7\,s^{-1}$ in MeOH ($\varepsilon = 32.7$); $k_1 = 16.4 \cdot 10^8\,s^{-1}$ and $k_2 = 6.5 \cdot 10^7\,s^{-1}$ in isopropanol ($\varepsilon = 18.9$); $k_1 = 9.14 \cdot 10^8\,s^{-1}$ and $k_2 = 5.1 \cdot 10^7\,s^{-1}$ in 1,4-dioxane ($\varepsilon = 2.0$).

Molecular modeling: Two conditions must be matched for energy transfer to occur. The first is a spectral requirement, that is, the emission spectrum of the donor must overlap the absorption spectrum of the acceptor, as shown in Figure 9 for

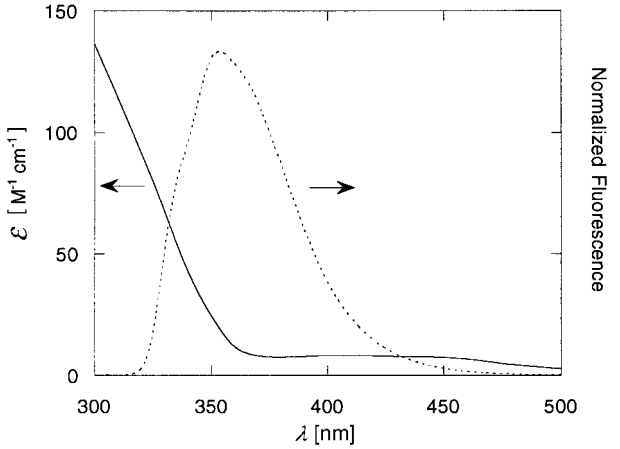

Figure 9. Spectral overlap between the normalized donor stimulated fluorescence, F_D (dashed line), and the acceptor extinction coefficient, ε (full line), for the Bin – TOAC hexapeptide.

the Bin – TOAC hexapeptide. The second condition is a geometric requirement: the emission and absorption dipoles of the donor and acceptor molecules, respectively, must be at an appropriate distance and properly oriented. Both these requirements are related to the transfer efficiency by Equation (12), where R_m is the center-to-center distance of the probes in the mth structure, κ_m^2 the corresponding orientation parameter, and R_0 the distance at which 50% transfer of excitation energy occurs. The values of R_0 in the different solvents used, as given by Equation (13),[40a] are reported in Table 5.

$$E_m = \frac{1}{1 + \left[\frac{2}{3\kappa_m^2}\left(\frac{R_m}{R_0}\right)^6\right]} \tag{12}$$

$$R_0 = 9.79 \cdot 10^3 [(2/3 \Phi_0 J_F)/n^4]^{-6} \tag{13}$$

To gather information on the geometric and steric constraints that control both the interchromophoric distance and probe orientation in the Bin – TOAC hexapeptide we have undertaken molecular mechanics calculations.[40b, c, 44] Briefly, we started by putting the backbone chain in both a left-handed (l.h.) and a right-handed (r.h.) 3_{10}-helix, and a l.h. and a r.h. α-helix as well as to explore all plausible conformations for the peptide main chain. The total energy of the mth structure was then evaluated by Equation (14),[40b,c] which comprises stretching and bending terms (STR and BEN), besides electrostatic (COUL), nonbonding (NB), and torsional (TOR) potentials similar to those previously employed by us.[40, 45]

$$U_{m,\,tot} = COUL + NB + TOR + STR + BEN \tag{14}$$

Because of the rigidity of the Bin – TOAC hexapeptide, we expected a rather narrow distribution of conformers for each backbone structure. In addition, the use of Equation (15) overcomes the uncertainty in the absolute value of the total energy arising from the empirical terms of Equation (14). In fact, ΔU_{tot} is the difference between the energy of the mth structure, $U_{m,\,tot}$, and the lowest energy among all structures of the peptide, U_{min} [Eq. (15)], which plays the role of a reference energy.

$$\Delta U_{tot} = U_{m,\,tot} - U_{min} \tag{15}$$

The most relevant computational results can be summarized as follows: a) A few sterically favored conformers are found, differing from each other by ≤ 2.5 kcal mol^{-1}, irrespective of the backbone screw sense and type of helical conformation, as shown in Table 7. Additional structures

Table 7. Conformers of the Bin – TOAC hexapeptide in the deepest energy minimum in methanol from molecular mechanics calculations.

Backbone conformation[a]	ΔU_{tot}[b] [kcal mol^{-1}]	R_m[c] [Å]	E_{calcd}[d]	E_{exp}[e]
l.h. 3_{10}-Helix[f]	0.0	5.84	0.74	0.72
	0.0	6.18	0.07	0.07
r.h. 3_{10}-Helix	1.7	8.69	0.67	
l.h. α-Helix	2.5	8.67	0.61	
r.h. α-Helix	1.1	7.35	0.89	

[a] Left-handed (l.h.) and right-handed (r.h.) helix. [b] From Equation (15). [c] Interchromophoric center-to-center distance. [d] Energy transfer efficiency; from Eq. (12). [e] Experimental transfer efficiency (E_1 and E_2, respectively); from Equation (2) and Table 4. [f] These two isoenergetic conformers differ in both center-to-center distance and mutual orientation of the chromophores (Table 6).

exhibit definitely higher energies, so that they can safely be neglected. b) Among the most probable structures, the most stable ones are two isoenergetic conformers with the backbone in the l.h. 3_{10}-helix (Figure 10). They differ for the spatial orientation of TOAC with respect to Bin, as a result of a different puckering of the TOAC moiety, as shown in Figure 11, where the values of the side chain torsion angles for TOAC in the crystal state are also reported. It is clear that the topologies of the TOAC ring structure in the computed conformations are close to those observed in the crystal state. c) Consistent with computational results, a comparison between the calculated [Eq. (12)] and experimental [Eq. (2)] transfer efficiencies, reported in Table 7, shows an excellent agreement only in the case of the two conformers with the backbone in the l.h. 3_{10}-helix (Figure 10). d) These two conformers are perturbed by the solvent, mainly affecting the mutual orientation of the chromophores (Table 6). In fact, in spite of the minor changes in the center-to-center distances ($\Delta R \sim 0.2$ Å), the quenching efficiencies between the two conformers markedly vary, because of the quite different values of the orientation factor κ_m^2, the κ_1^2/κ_2^2 ratio ranging from 11.3 to 25.7 in the different solvents used. This

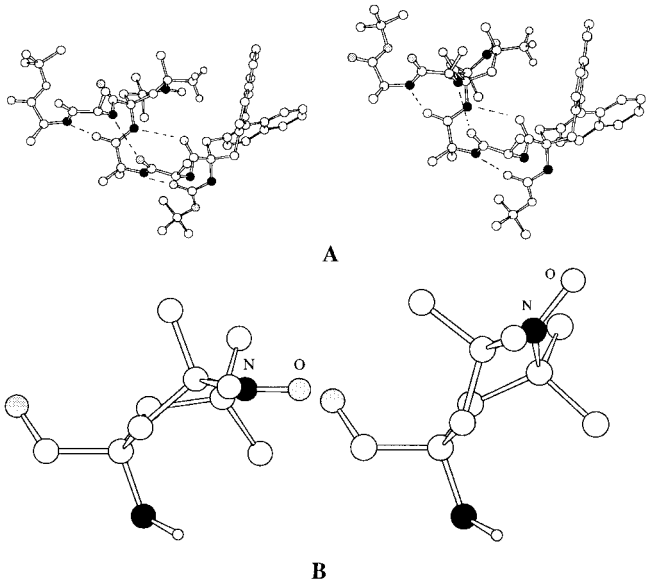

Figure 10. Molecular models of the two most stable solution conformations for the Bin – TOAC hexapeptide A), and topology of TOAC moiety in the two conformers (B; see Figure 11). The peptide backbone is in the left-handed 3_{10}-helix [viewed perpendicularly to the helical axis in A), where the four intramolecular H-bonds are indicated by dashed lines]. Nitrogen atoms are in black and oxygen atoms are in grey. Note in A) the close approach of one methyl group of TOAC to one naphthyl moiety of Bin, causing the chromophores to experience C–H $\cdots$ π interactions that stiffen the whole molecule.

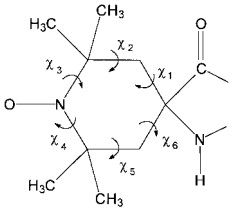

Conformer	χ_1	χ_2	χ_3	χ_4	χ_5	χ_6
X-ray (Mol. **A**)	3.9	– 43.0	41.7	1.7	– 46.7	43.4
X-ray (Mol. **B**)	20.4	– 48.0	24.0	24.7	– 55.2	33.2
Computed **1**	– 15.0	– 33.0	48.3	– 12.0	– 40.4	53.4
Computed **2**	24.5	– 51.3	22.0	28.9	– 57.3	30.2

Figure 11. Side-chain torsion angles of TOAC in the two conformations in the crystal state and in solution, according to the X-ray diffraction and molecular mechanics data, respectively. In both cases, the peptide backbone is in the left-handed 3_{10}-helical structure.

conclusion is consistent with the observation that also the preexponents α_i, which measure the relative population of the species undergoing energy transfer, change somewhat with the solvent (Table 4). e) The angle between the transition moment of TOAC and the total dipole moment of the helix (Figure 6) is very close to 90° for both conformers, which implies a definitely minor effect of the electrostatic potential generated by the helical arrangement[41] on the energy-transfer process.[13]

Since the calculated efficiency comprises the solvent-dependent parameter R_0, the excellent agreement between calculated and experimental efficiencies makes it reasonable to consider the two computed conformations reported in Figure 10 as a good representation of the actual structures present in solution. Their conformational rigidity partly arises from the steric proximity between one TOAC methyl group and one Bin naphthyl moiety (see the crystal-state structure discussed above), which stiffens the whole molecule. Change in backbone screw sense and/or conformation perturbs these geometric features; this causes the chromophores, and the whole molecule as well, to acquire some conformational mobility, but the ensuing gain in molecular entropy is apparently overcompensated by an increase in energy, leading to less stable structures. This is accounted for by the fluorescence decay results, which clearly indicate that in solution only the two conformers illustrated in Figure 10 exist, which exhibit structural features similar to those found in the crystal state.

Conclusion

Combination of X-ray diffraction and (steady-state and time-decay) fluorescence data with results from molecular mechanics calculations was productive in determining the structural and photophysical properties of the first peptide-based, rigid donor – spacer – acceptor system. In solution, the molecules preserve the ordered secondary structure, including type and handedness of the helix formed observed in the crystal state. In summary, this work strongly supports the view that the exploitation of severely conformationally restricted C^{α}-tetrasubstituted α-amino acids (such as the Aib, Ac_nc, Bin and TOAC residues discussed here) ideally enables an easy synthesis of rigid interchromophoric spacers of variable intercomponent geometries and concomitantly allows for a detailed investigation of through-space interactions between rigid photoactive probes.

Experimental Section

Peptide synthesis: The synthesis and characterization of Boc-(*S*)-Bin-O*t*Bu[17b] (blank) and Fmoc-Ala-Aib-TOAC-(Ala)$_2$-O*t*Bu (Fmoc, 9-fluorenylmethyloxycarbonyl)[15c] have already been reported. The Fmoc N^{α}-protecting group of the pentapeptide was removed by treatment with a 20% diethylamine solution in acetonitrile. After evaporation of the solvent, the N^{α}-deprotected peptide was dissolved in $CHCl_3$ and isolated by elution through a 3 cm bed of silica gel with $CHCl_3$/EtOH 8:2. Boc-(*S*)-Bin-OH[17b] was subsequently incorporated into the pentapeptide with 1-[3-(dimethylamino)propyl]-3-ethylcarbodiimide hydrochloride (EDC · HCl) and 7-aza-1-hydroxy-1,2,3-benzotriazole[46] (HOAt) in CH_2Cl_2. The terminally protected Bin – TOAC hexapeptide was purified by flash chromatography with $CHCl_3$/EtOH 96:4 and recrystallized from ethyl acetate/light petroleum. Yield 73%; m.p. 249 – 250 °C; TLC (Kieselgel 60 F_{254} plates; Merck): R_{f1}($CHCl_3$/EtOH 9:1) 0.95; R_{f2}(toluene/EtOH 7:1) 0.30; $[\alpha]_D^{20}$: – 59.3° ($c = 0.1$, methanol); IR absorption (KBr): 3324, 1724, 1665, 1524 cm^{-1}.

X-ray diffraction: Clear colorless crystals were grown from acetone/light petroleum by vapor diffusion. Crystal data and refinement parameter information are given in Table 8. Diffraction data were collected on a computer-controlled Bruker 1 K Smart CCD system with a 5 kW Rigaku rotating anode source and Göbel mirrors. Unit cell dimensions were determined by a least-squares refinement of 306 centered reflections within $-41 < 2\theta < 78°$. Data collection nominally covered a hemisphere in reciprocal space by combining six sets of exposures with different 2θ and φ angles: each exposure covered a range of 0.25° in ω. The crystal-to-detector distance was 5.05 cm. Data were collected to 0.9 Å resolution and a repetition of 60 of the initial frames at the end of the data set showed that the crystal remained stable during data collection. An empirical absorption

  0947-6539/99/0508-2262 $ 17.50+.50/0 *Chem. Eur. J.* **1999**, *5*, No. 8

Table 8. Crystal data and structure refinement for the Bin – TOAC hexapeptide.

empirical formula [amu]	$2(C_{56}H_{74}N_7O_{10})\cdot C_3H_6O$	
formula weight	2068.5	
temperature [K]	293(2)	
wavelength [Å]	1.5418	
crystal system	monoclinic	
space group	$P2_1$	
unit cell dimensions	$a = 13.813(1)$	$\alpha = 90^\circ$
	$b = 26.388(3)$	$\beta = 101.26(1)^\circ$
	$c = 17.936(2)$	$\gamma = 90^\circ$
volume [Å^3]	6412(1)	
Z	2	
density (calcd) [Mg m^{-3}]	1.07	
absorption coefficient [mm^{-1}]	0.60	
$F(000)$	2220	
crystal size [mm]	$0.38 \times 0.33 \times 0.28$	
Θ range for data collection [°]	3.02 to 58.87	
index ranges	$-14 \le h \le 13$, $-24 \le k \le 29$, $-19 \le 1 \le 19$	
reflns collected	21879	
independent reflections	12936 [R(int) = 0.038]	
refinement method	full-matrix least-squares on F^2	
data/restraints/parameters	12936/27/1364	
goodness-of-fit (on F^2)	1.1	
final R indices [$I > 2\sigma(I)$]	$R1 = 0.050$, $wR2 = 0.131$	
R indices (all data)	$R1 = 0.058$, $wR2 = 0.140$	
largest diff. peak and hole [e Å^{-3}]	0.349; −0.265	

correction was calculated with program SADABS[47a] which uses equivalent reflections to calculate absorption effects.

The structure was solved by the Shake and Bake (SnB V1.5) direct-phasing program[47b] with E values generated by XTAL V3.2.[47c] Eleven hundred trial structures were calculated and subjected to 75 cycles of iterative structure factor calculations, phase refinement, and density modification. Only one trial, with a minimal function value[47d, e] of 0.37, gave a solution for the structure. The minimal function values for the incorrect structures ranged from 0.43 to 0.47. The structure was refined with the SHELXL-97 program.[47f] There were two peptide molecules and one acetone (solvent) molecule in the asymmetric unit. The 1364 refined parameters included coordinates and anisotropic thermal parameters for all nonhydrogen atoms. Hydrogens were refined by means of a riding model. The acetone molecule was disordered over three positions with occupancy ratios 65:20:15. The two minor acetone molecules were constrained to be flat (nonhydrogen atoms) and to have the same bonds and angles as the major acetone molecule.

Crystallographic data (excluding structure factors) for the structure reported in this paper have been deposited within the Cambridge Crystallographic Data Centre as supplementary publication no. CCDC-114992. Copies of the data can be obtained free of charge on application to CCDC, 12 Union Road, Cambridge CB2 1EZ, UK [Fax: (+44) 1223-336-033; e-mail: deposit@ccdc.cam.ac.uk].

UV absorption and fluorescence: Ultraviolet absorption spectra were obtained on a JASCO 7850 spectrophotometer. Steady-state fluorescence spectra were recorded on a SPEX Fluoromax spectrofluorimeter operating in the SPC mode. Quantum yields were evaluated with respect to naphthalene in cyclohexane ($\Phi_S = 0.22$). Nanosecond decays were measured by a CD900 SPC lifetime apparatus from Edinburgh Instruments. Excitation in the UV region was achieved by a coaxial flash lamp filled with ultrapure hydrogen (0.3 atm) and driven at 30 kHz of repetition rate. The resulting excitation profile, recorded through a diluted scattering solution of glycogen, has FWHM = 1.2 ns. The decay curves were fitted by a nonlinear, least-squares analysis to exponential functions by an iterative deconvolution method. All experiments were carried out in quartz cells, using solutions previously bubbled with ultrapure nitrogen for 20 min. Distribution analysis of the time decays was also performed in a number of solvents. Other instrumentation has already been described.[48]

Molecular mechanics calculations: In-house programs, already used in our group for the last 15 years, but with equation parameters continuously improved,[40, 45, 48] were employed to calculate nonbonding, electrostatic, hydrogen bonding and torsional potentials, by making use of the appropriate partial charges[45] for each atom in the compounds. The energy minimization procedure, based on the conjugated gradient, was initially performed maintaining both bond lengths and bond angles fixed. The deepest energy minimum structures were then further refined by relaxing the rigid geometry and taking into account the standard stretching and bending terms,[44] thus providing the final energy minima according to Equation (14).

[1] P. Wu, L. Brand, *Anal. Biochem.* **1994**, *218*, 1 – 13.
[2] S. Speiser, *Chem. Rev.* **1996**, *96,* 1953 – 1976.
[3] a) L. Stryer, R. P. Haugland, *Proc. Natl. Acad. Sci. USA* **1967**, *58*, 719 – 726; b) E. Haas, E. Katchalski-Katzir, I. Z. Steinberg, *Biopolymers* **1978**, *17*, 11 – 31.
[4] a) S. S. Isied, A. Vassilian, *J. Am. Chem. Soc.* **1984**, *106*, 1732 – 1736; b) M. Faraggi, M. H. Klapper, *J. Chim. Phys. Physicochim. Biol.* **1991**, *88*, 1009 – 1019; c) M. Y. Ogawa, I. Moreira, J. F. Wishart, S. S. Isied, *Chem. Phys.* **1993**, *176*, 589 – 600; d) M. Y. Ogawa, J. F. Wishart, Z. Young, J. R. Miller, S. S. Isied, *J. Phys. Chem.* **1993**, *97*, 11 456 – 11 463; e) H. Tamiaki, K. Nomura, K. Maruyama, *Bull. Chem. Soc. Jpn.* **1994**, *67*, 1863 – 1871; f) A. K. Mishra, R. Chandrasekar, M. Faraggi, M. H. Klapper, *J. Am. Chem. Soc.* **1994**, *116*, 1414 – 1422; g) T. Hayashi, T. Takimura, J. Hitomi, T. Ohara, H. Ogoshi, *J. Chem. Soc. Chem. Commun.* **1995**, 545 – 546; h) G. Jones II, L. N. Lu, V. Vullev, D. J. Gosztola, S. R. Greenfield, M. R. Wasilievski, *Bioorg. Med. Chem. Lett.* **1995**, *5*, 2385 – 2390; i) N. Voyer, J. Lamothe, *Tetrahedron* **1995**, *51*, 9241 – 9284.
[5] a) C. M. K. Nair, M. Vijayan, *J. Indian Inst. Sci.* **1981**, *63C*, 81 – 103; b) E. Benedetti, A. Bavoso, B. Di Blasio, V. Pavone, C. Pedone, C. Toniolo, G. M. Bonora, *Biopolymers* **1983**, *22*, 305 – 317; c) A. Yaron, F. Naider, *CRC Crit. Rev. Biochem.* **1993**, *28*, 31 – 81.
[6] a) C. Toniolo, G. M. Bonora, V. N. R. Pillai, M. Mutter, *Macromolecules* **1986**, *13*, 772 – 774; b) M. Goodman, C. Toniolo, P. Pallai in *Forum Peptides* (Eds.: B. Castro, J. Martinez), Dohr, Nancy, **1986**, pp. 146 – 174.
[7] a) M. Goodman, A. S. Verdini, C. Toniolo, W. D. Phillips, F. A. Bovey, *Proc. Natl. Acad. Sci. USA* **1967**, *64*, 444 – 450; b) C. Toniolo, G. M. Bonora, *Makromol. Chem.* **1975**, *176*, 2547 – 2558; c) C. Toniolo, G. M. Bonora, M. Mutter, *J. Am. Chem. Soc.* **1979**, *101*, 450 – 454.
[8] C. Toniolo, E. Benedetti, *Macromolecules* **1991**, *24*, 4004 – 4009.
[9] a) G. R. Marshall in *Intra-Science Chemical Reports Vol. 5,* (Ed.: N. Kharasch), Gordon and Breach, New York, **1971**, pp. 305 – 316; b) I. L. Karle, P. Balaram, *Biochemistry* **1990**, *29*, 6747 – 6756.
[10] a) C. M. Venkatachalam, *Biopolymers* **1968**, *6*, 1425 – 1436; b) C. Toniolo, *CRC Crit. Rev. Biochem.* **1980**, *9*, 1 – 44; c) G. D. Rose, L. M. Gierasch, J. A. Smith, *Adv. Protein Chem.* **1985**, *37*, 1 – 109.
[11] C. Toniolo, E. Benedetti, *Trends Biochem. Sci.* **1991**, *16*, 350 – 353.
[12] a) G. Basu, K. Bagchi, A. Kuki, *Biopolymers* **1991**, *31*, 1763 – 1774; b) G. Basu, A. Kuki, *Biopolymers* **1992**, *32*, 61 – 71; c) G. Basu, M. Kubasik, D. Anglos, A. Kuki, *J. Phys. Chem.* **1993**, *97*, 3956 – 3967; d) G. Basu, D. Anglos, A. Kuki, *Biochemistry* **1993**, *32*, 3067 – 3076; e) V. A. Bindra, A. Kuki, *Int. J. Pept. Protein Res.* **1994**, *44*, 539 – 548; f) D. Anglos, V. Bindra, A. Kuki, *J. Chem. Soc. Chem. Commun.* **1994**, 213 – 215.
[13] a) E. Galoppini, M. A. Fox, *J. Am. Chem. Soc.* **1996**, *118*, 2299 – 2300; b) T. L. Batchelder, R. J. Fox III, M. S. Meier, M. A. Fox, *J. Org. Chem.* **1996**, *61*, 4206 – 4209; c) M. A. Fox, E. Galoppini, *J. Am. Chem. Soc.* **1997**, *119*, 5277 – 5284.
[14] a) F. Donald, G. Hungerford, D. J. S. Birch, B. D. Moore, *J. Chem. Soc. Chem. Commun.* **1995**, 313 – 314; b) G. Hungerford, M. Martinez-Insua, D. J. S. Birch, B. D. Moore, *Angew. Chem.* **1996**, *108*, 356 – 359; *Angew. Chem. Int. Ed. Engl.* **1996**, *35*, 326 – 329.
[15] a) C. Toniolo, E. Valente, F. Formaggio, M. Crisma, G. Pilloni, C. Corvaja, A. Toffoletti, G. V. Martinez, M. P. Hanson, G. L. Millhauser, C. George, J. L. Flippen-Anderson, *J. Pept. Sci.* **1995**, *1*, 45 – 57; b) P. Hanson, G. Martinez, G. Millhauser, F. Formaggio, M. Crisma, C. Toniolo, C. Vita, *J. Am. Chem. Soc.* **1996**, *118*, 271 – 272; c) P. Hanson, G. Millhauser, F. Formaggio, M. Crisma, C. Toniolo, *J. Am. Chem. Soc.* **1996**, *118*, 7618 – 7625; d) J. L. Flippen-Anderson, C. George, G. Valle, E. Valente, A. Bianco, F. Formaggio, M. Crisma, C. Toniolo, *Int. J. Pept. Protein Res.* **1996**, *47*, 231 – 238; e) M. Crisma, V. Monaco, F. Formaggio, C. Toniolo, C. George, J. L. Flippen-Anderson, *Lett. Pept. Sci.* **1997**, *4*, 213 – 218.

[16] L. P. McMahon, H. T. Yu, M. A. Vela, G. A. Morales, L. Shui, F. R. Fronczek, M. L. McLaughlin, M. D. Barkley, *J. Phys. Chem.* **1997**, *B101*, 3269 – 3280.
[17] a) J.-P. Mazaleyrat, A. Gaucher, M. Wakselman, L. Tchertanov, J. Guilhem, *Tetrahedron Lett.* **1996**, *37*, 2971 – 2974; b) J.-P. Mazaleyrat, A. Gaucher, J. Savrda, M. Wakselman, *Tetrahedron: Asymmetry* **1997**, *8*, 619 – 631; c) A. Peter, G. Torok, J.-P. Mazaleyrat, M. Wakselman, *J. Chromatogr.* **1997**, *A789*, 41 – 46; d) J.-P. Mazaleyrat, A. Boutboul, Y. Lebars, A. Gaucher, M. Wakselman, *Tetrahedron: Asymmetry* **1998**, *9*, 2701 – 2713.
[18] IUPAC-IUB Commission on Biochemical Nomenclature, *J. Mol. Biol.* **1970**, *52*, 1.
[19] E. Benedetti, C. Pedone, C. Toniolo, G. Némethy, M. S. Pottle, H. A. Scheraga, *Int. J. Pept. Protein Res.* **1980**, *16*, 156 – 172.
[20] W. B. Schweizer, J. D. Dunitz, *Helv. Chim. Acta* **1982**, *65*, 1547 – 1554.
[21] a) E. Benedetti in *Chemistry and Biochemistry of Amino Acids, Peptides and Proteins Vol. 6,* (Ed.: B. Weinstein), Dekker, New York, **1982**, pp. 105 – 184; b) T. Ashida, Y. Tsunogae, I. Tanaka, T. Yamane, *Acta Crystallogr.* **1987**, *B43*, 212 – 218.
[22] a) Y. Paterson, S. M. Rumsey, E. Benedetti, G. Némethy, H. A. Scheraga, *J. Am. Chem. Soc.* **1981**, *103*, 2947 – 2955; b) G. Valle, M. Crisma, F. Formaggio, C. Toniolo, G. Jung, *Liebigs Ann.* **1985**, 1055 – 1060.
[23] a) C. Ramakrishnan, N. Prasad, *Int. J. Protein Res.* **1971**, *3*, 209 – 231; b) R. Taylor, O. Kennard, W. Versichel, *Acta Crystallogr.* **1984**, *B40*, 280 – 288; c) C. H. Görbitz, *Acta Crystallogr.* **1989**, *B45*, 390 – 395.
[24] S. S. Zimmerman, M. S. Pottle, G. Némethy, H. A. Scheraga, *Macromolecules* **1977**, *10*, 1 – 9.
[25] C. Toniolo, E. Benedetti in *Molecular Conformation and Biological Interactions* (Eds.: P. Balaram, S. Ramaseshan), Indian Academy of Sciences, Bangalore, India, **1991**, pp. 511 – 521.
[26] J. D. Dunitz, P. Strickler in *Structural Chemistry and Molecular Biology* (Eds.: A. Rich, N. Davidson), Freeman, San Francisco, **1968**, pp. 595 – 602.
[27] D. Cremer, J. A. Pople, *J. Am. Chem. Soc.* **1975**, *97*, 1354 – 1358.
[28] F. H. Allen, J. A. K. Howard, N. A. Pitchford, *Acta Crystallogr.* **1993**, *B49*, 910 – 928.
[29] T. Förster, *Discuss. Faraday Soc.* **1959**, *27*, 7 – 17.
[30] G. D. Scholes, K. P. Ghiggino, A. M. Oliver, M. N. Paddon-Row, *J. Am. Chem. Soc.* **1993**, *115*, 4345 – 4349.
[31] B. Pispisa, F. Cavalieri, M. Venanzi, A. Sisto, *Biopolymers* **1996**, *40*, 529 – 542.
[32] a) E. London, *Mol. Cell. Biochem.* **1982**, *45*, 181 – 187; b) A. P. Winiski, M. Eisenberg, A. Chattopadhyay, E. London, *Biochemistry* **1987**, *26*, 39 – 47; c) E. Asuncion-Punzalan, E. London, *Biochemistry* **1995**, *34*, 11460 – 11466; d) M. Langner, S. McLaughlin, *Biochemistry* **1988**, *27*, 386 – 392; e) M. Castanho, M. Prieto, *Biophys. J.* **1995**, *69*, 155 – 168; f) J. S. Puskin, A. L. Vistnes, M. T. Coene, *Arch. Biochem. Biophys.* **1981**, *206*, 164 – 172.
[33] a) J. A. Green, L. A. Singer, J. H. Parks, *J. Chem. Phys.* **1973**, *58*, 2690 – 2695; b) S. A. Green, D. J. Simpson, G. Zhou, P. S. Ho, N. V. Blough, *J. Am. Chem. Soc.* **1990**, *112*, 7337 – 7346; c) V. A. Kuzmin, A. S. Tatikolov, *Chem. Phys. Lett.* **1977**, *51*, 45 – 47.
[34] a) J. Matko, K. Ohki, M. Edidin, *Biochemistry* **1992**, *31*, 703 – 711; b) J. Matko, A. Jenei, L. Matyus, M. Ameloot, S. Damjanovich, *Photochem. Photobiol. B* **1993**, *19*, 69 – 73; c) J. Matko, A. Jenei, T. Wei, M. Edidin, *Cytometry* **1995**, *19*, 191 – 200.
[35] a) J. Karpiuk, R. Grabowski, *Chem. Phys. Lett.* **1989**, *160*, 451 – 456; b) S. K. Chattopadhyay, P. K. Das, G. L. Hug, *J. Am. Chem. Soc.* **1983**, *105*, 6205 – 6210; c) W. A. Yee, V. A. Kuzmin, D. S. Kliger, G. S. Hammond, A. J. Twarowski, *J. Am. Chem. Soc.* **1979**, *101*, 5104 – 5106.
[36] a) S. S. Atik, L. A. Singer, *J. Am. Chem. Soc.* **1978**, *100*, 3234 – 3235; b) J. C. Scaiano, C. I. Paraskevopoulos, *Can. J. Chem.* **1984**, *62*, 2351 – 2354.
[37] T. Förster, *Ann. Phys.* (*Leipzig*) **1948**, *2*, 55 – 75.
[38] D. L. Dexter, *J. Chem. Phys.* **1953**, *21*, 836 – 850.
[39] a) I. Z. Steinberg, *J. Chem. Phys.* **1968**, *48*, 2411 – 2413; b) A. Grinvald, E. Haas, I. Z. Steinberg, *Proc. Natl. Acad. Sci. USA* **1972**, *69*, 2273 – 2277.
[40] a) B. Pispisa, A. Palleschi, M. Venanzi, G. Zanotti, *J. Phys. Chem.* **1996**, *100*, 6835 – 6844; b) B. Pispisa, M. Venanzi, A. Palleschi, G. Zanotti, *J. Photochem. Photobiol. A: Chem.* **1997**, *105*, 225 – 233; c) B. Pispisa, A. Palleschi, M. E. Amato, A. L. Segre, M. Venanzi, *Macromolecules* **1997**, *30*, 4905 – 4910.
[41] W. G. J. Hol, P. T. van Duijnen, H. J. C. Berendesen, *Nature*, **1978**, *273*, 443 – 446.
[42] G. D. Scholes, K. P. Ghiggino, *J. Phys. Chem.* **1994**, *98*, 4580 – 4590.
[43] S. Speiser, J. Katriel, *Chem. Phys. Lett.* **1983**, *102*, 88 – 94.
[44] a) N. L. Allinger, *J. Am. Chem. Soc.* **1977**, *99*, 8127 – 8134; b) J. Burkert, N. L. Allinger in *Molecular Mechanics*, ACS, Washington, DC, **1982**.
[45] a) B. Pispisa, A. Palleschi, M. Barteri, S. Nardini, *J. Phys. Chem.* **1985**, *89*, 1767 – 1775; b) B. Pispisa, A. Palleschi, G. Paradossi, *J. Phys. Chem.* **1987**, *91*, 1546 – 1553; c) B. Pispisa, G. Paradossi, A. Palleschi, A. Desideri, *J. Phys. Chem.* **1988**, *92*, 3422 – 3429; d) G. Paradossi, E. Chiessi, M. Venanzi, B. Pispisa, A. Palleschi, *Int. J. Biol. Macromol.* **1992**, *14*, 73 – 80; e) E. Chiessi, M. Branca, A. Palleschi, B. Pispisa, *Inorg. Chem.* **1995**, *34*, 2600 – 2609.
[46] L. A. Carpino, *J. Am. Chem. Soc.* **1993**, *115*, 4397 – 4398.
[47] a) G. M. Sheldrick, *SADABS*, *Absorption Correction Program*, University of Göttingen, Göttingen, Germany, **1995**; b) R. Miller, S. M. Gallo, H. G. Khalak, C. M. Weeks, *J. Appl. Crystallogr.* **1994**, *27*, 613 – 621; c) S. Hall, V. Subramanian, *GENEV Xtal 3.2 Reference Manual* (Eds.: S. R. Hall, H. D. Flack, J. M. Stewart), Universities of Western Australia, Geneva, and Maryland, Lamb, Perth, Australia, **1992**; d) C. M. Weeks, G. T. De Titta, R. Miller, H. A. Hauptman, *Acta Crystallogr.* **1993**, *D49*, 179 – 181; e) C. M. Weeks, G. T. De Titta, H. A. Hauptman, P. Thuman, R. Miller, *Acta Crystallogr.* **1994**, *A50*, 210 – 220; f) G. M. Sheldrick, *SHELXL 93*, *Program for Refinement of Crystal Structures*, University of Göttingen, Göttingen, Germany, **1997**.
[48] B. Pispisa, M. Venanzi, A. Palleschi, G. Zanotti, G. *Macromolecules* **1994**, *27*, 7800 – 7808.

Received: November 12, 1998 [F1437]

  0947-6539/99/0508-2264 $ 17.50+.50/0